to give any improvement. Bond angles and separations resulting from these hydrogen positions are found in Table 6. Attempts to grow a crystal large enough for a neutron diffraction study have so far failed.

References

ABRAHAMS, S. C. & REDDY, J. M. (1965). *J. Chem. Phys.* **43**, 2533.

BERGHUIS, J., HAANAPPEL, IJ. M., POTTERS, M., LOOPSTRA, B. O., MACGILLAVRY, C. H. & VEENENDAAL, A. L. (1955). *Acta Cryst.* **8**, 478.

BILTZ, W. & BIRK, E. (1925). *Z. anorg. Chem.* **150**, 20.

BUSING, W. R., MARTIN, K. O. & LEVY, H. A. (1962). ORNL-TM-305, Oak Ridge, National Laboratory Oak Ridge, Tennessee.

DANCE, I. G. & FREEMAN, H. C. (1965). *J. Inorg. Chem.* **4**, 1555.

DAWSON, B. (1960). *Acta Cryst.* **13**, 403.

FREEMAN, A. J. & WATSON, R. E. (1961). *Acta Cryst.* **14**, 231.

IBERS, J. A. & CROMER, D. T. (1958). *Acta Cryst.* **11**, 794.

International Tables for X-ray Crystallography (1962). Vol. III, p.213. Birmingham: Kynoch Press.

MOROSIN, B. (1964). Unpublished.

MOROSIN, B. (1965). Program and Abstracts, Amer. Cryst. Assoc. Meeting, Gatlinburg, Tennessee; paper B-4.

STEWART, J. M. & HIGH, D. F. (1964). Program and Abstracts, Amer. Cryst. Assoc. Meeting, Bozeman, Montana; paper B-13.

TEMPLETON, D. H. (1955). *Acta Cryst.* **8**, 842.

THOMAS, L. H. & UMEDA, K. (1957). *J. Chem. Phys.* **26**, 293.

WEHE, D. J., BUSING, W. R. & LEVY, H. A. (1962). ORNL-TM-229, Oak Ridge National Laboratory, Oak Ridge, Tennessee.

Acta Cryst. (1966). **21**, 284

X-ray diffraction topographs of an elastically distorted crystal.

By YOSHINORI ANDO and NORIO KATO, *Department of Applied Physics, Faculty of Engineering, Nagoya University, Nagoya, Japan*

(*Received* 24 *December* 1965)

Dynamical diffraction phenomena of X-rays are very important for understanding lattice distortion in nearly perfect crystals. This preliminary report concerns the diffraction topographs observed in an elastically distorted crystal of silicon.

The original specimen was nearly free from dislocations, oxygen bands and other lattice distortions. The form of the specimen was a circular disk 8 mm in diameter and 1·4 mm thick. The disk surfaces were parallel to the ($\bar{1}11$) plane. A diametrical compression was applied to the crystal, as shown schematically in Fig. 1. The method of applying the force was similar to that used in the X-ray topograph work of Fukushima, Hayakawa & Nimura (1962, 1963). However, the positional resolution of the present topograph patterns was highly increased by the use of Lang's (1959) technique. Moreover, section-type topographs were also studied (Kato & Lang, 1959). The topographs obtained by Lang's technique are called the traverse patterns, hereafter. The X-ray radiation was $A_gK\alpha_1$.

In Fig. 2 a traverse pattern of the 220 reflexion is shown, the net plane here being perpendicular to the applied force. The diffraction condition is also illustrated in Fig. 2(*b*). *P* indicates the position at which the force was applied to the crystal. The total force was measured by a strain gauge and was a few kilograms in this case. Here, the following points are noticeable:

(*a*) Fringe patterns are recognized in a wide region (*F*) far from the point *P*.

(*b*) Close to *P*, there is a circular region (*E*) which has a very strong reflecting power.

(*c*) In the neighbourhood of the region *E*, a region (*G*) of fairly strong intensity spreads upwards and downwards.

(*d*) On the left side of the region *E*, between *E* and *F*, there is a region (*D*) which reflects X-rays strongly. Precisely speaking, the region *D* overlaps the region *F* to some extent.*

(*e*) If the reflecting condition is reversed, namely the $\bar{2}\bar{2}0$ reflexion is used, the reflecting power of the region *D* becomes less than that of the perfect crystal (departure from Friedel's law).

(*f*) On the other hand, the observations (*a*), (*b*) and (*c*) are not changed essentially when the reflexion condition is reversed.

(*g*) When the force applied at *P* is decreased, the regions *D*, *E*, *F* and *G* contract towards *P*. Even when the wedge *W* contacts the crystal with a force less than 100 grams, a tiny dark spot still remains near *P*, with very faint fringes.

The crystal, upon release from the force, shows the pattern of a perfect crystal, so that all the phenomena described above are caused by elastic distortion. The phenomena (*d*) and (*e*) have already been observed by Fukushima *et al.*

In order to understand the diffraction phenomena in more detail, the section topographs were studied with a very narrow flat pencil of X-rays. A few examples are given in Fig. 3. Positions at which the section topographs were taken are indicated by the arrows in Fig. 2. The magnitude of the

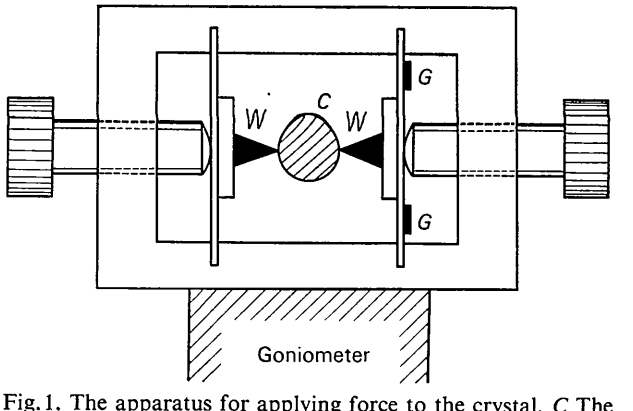

Fig. 1. The apparatus for applying force to the crystal. *C* The specimen. *W* The wedge-shaped block. *G* The elements of the strain gauge.

* In the present case, the force is applied in a slightly asymmetrical way with respect to the net plane.

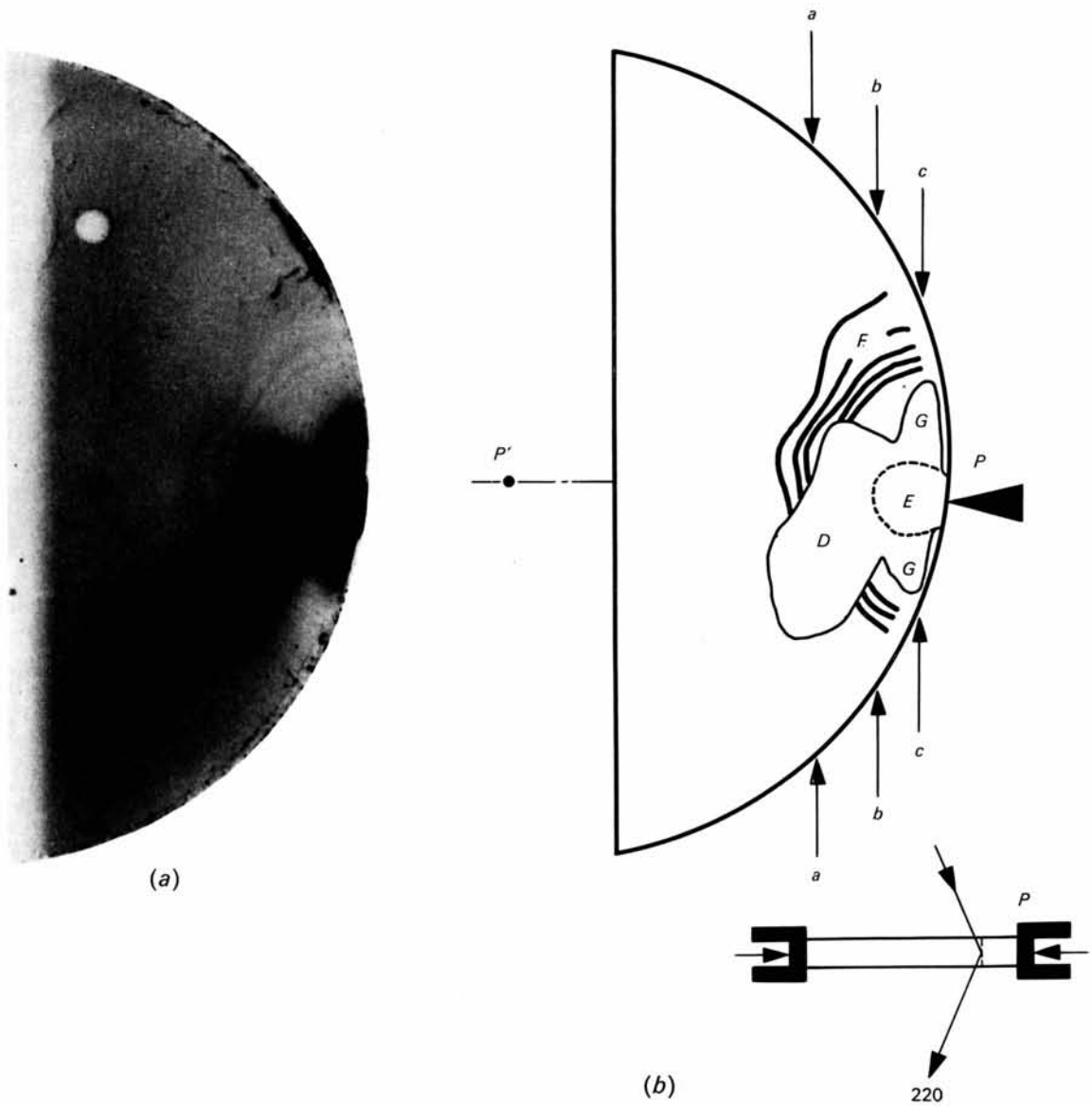

Fig. 2. (*a*) The traverse pattern of the crystal under compression. (*b*) Schematic illustration of (*a*). The regions *D*, *E*, *F* and *G* are explained in the text. The arrows *a*, *b* and *c* indicate the positions at which the section patterns were taken. The drawing at bottom-right shows the condition of reflexion.

[*To face p.* 284

a b c

Fig. 3. The section patterns corresponding to Fig. 2.

applied force and the net plane used were the same for Fig. 3 as for Fig. 2.

Position *a* covers the regions *F* and *D*. Elliptic and hook-shaped fringes are recognized, although a parallel-sided crystal was used. Similar ones appear also in the top and bottom parts of sections *b* and *c*. Incidentally, if the crystal is in the shape of a parallel slab and undistorted, a system of parallel fringes should be expected (Kato, 1961*a*, *b*; Authier & Lang, unpublished). The appearance of non-parallel fringes is understandable by the dynamical diffraction theory on slightly deformed crystals (Kato, 1963, 1964*a*, *b*). According to the theory, the fringe distance should decrease with increase of the strain gradient.* In fact, the fringe position is determined by an effective thickness Z which is proportional to the real thickness and the strain gradient (*cf.* equation (30) of Kato, 1964*b*). Since the strain gradient is maximum on the central line PP' of Fig. 2 in every column section of the crystal, higher order fringes will spring up from the central part of the section pattern. In other words, the central part is effectively thick. Since the fringes in the traverse pattern are essentially the loci of the apices of the hook-shaped and elliptic fringes, they may be called the 'fringes of equal strain-gradient', just as the terms 'equal thickness fringes' and 'equal inclination fringes' are used in electron microscopy. The fact that the behaviour of fringe phenomena is the same for the hkl and $\bar{h}\bar{k}l$ reflexions is also expected from the theory.

The dark background in the section pattern *a* accounts for the appearance of the region *D* in the traverse pattern. In general, the darkness of traverse patterns corresponds to the integrated intensity of crystals. The enhancement of the integrated intensity in distorted crystals is expected from the previous theory (Kato, 1964*b*). According to the theory, however, the departure from Friedel's law can not be expected unless the Borrmann absorption is taken into account. In the case of our region *D* the Borrmann absorption has nothing to do with the observation, because the sign of the indices for the net plane in which the enhancement is observed is opposite to the sign predicted by the theory under the experimental conditions described above.

In the central part of section pattern *b*, a broad line of high intensity is recognized. This broad line appears also in section pattern *c*. From the geometrical correspondence between the section and traverse patterns we know that the region *G* corresponds to the central broad line in the section pattern. For this reason the regions *D* and *G* were distinguished above, although they look similar in the traverse pattern so far as the intensity is concerned.

Finally, in section pattern *c*, a pair of dark images appears on either side of the central dark line. In pattern *b* the corresponding one is recognized markedly only on the right side of the central line. These pair images correspond to the region *E* in the traverse pattern.

In conclusion, the fringe phenomena can be explained by assuming the contraction of fringe distance in distorted crystals. The contraction has been predicted theoretically. The regions *D*, *E* and *G* can not be understood straightforwardly by the previous theory.

* Although the conclusion was derived in the special case of homogeneous bending, it can be shown that the theory is applicable correctly to any type of small distortion in which the displacement can be represented in a quadratic form of coordinates (Kato & Ando, 1966).

References

FUKUSHIMA, E., HAYAKAWA, K. & NIMURA, H. (1962). *J. Phys. Soc. Japan* **17**, 709.

FUKUSHIMA, E., HAYAKAWA, K. & NIMURA, H. (1963). *J. Phys. Soc. Japan*, Supplement II, **18**, 348.

KATO, N. (1961*a*). *Acta Cryst.* **14**, 526.

KATO, N. (1961*b*). *Acta Cryst.* **14**, 627.

KATO, N. (1963). *J. Phys. Soc. Japan*, **18**, 1785.

KATO, N. (1964*a*). *J. Phys. Soc. Japan*, **19**, 67.

KATO, N. (1964*b*). *J. Phys. Soc. Japan*, **19**, 971.

KATO, N. & ANDO, Y. (1966). *J. Phys. Soc. Japan.* **21**, 964.

KATO, N. & LANG, A. R. (1959). *Acta Cryst.* **12**, 249.

LANG, A. R. (1959). *Acta Cryst.* **12**, 787.

Acta Cryst. (1966). **21**, 285

Bond lengths and thermal vibrations in *m*-dinitrobenzene.

BY JAMES TROTTER* and C. S. WILLISTON, *Department of Chemistry, University of British Columbia, Vancouver* 8, *B.C., Canada*

(*Received* 9 *August* 1965 *and in revised form* 22 *January* 1966)

X-ray analysis of *m*-dinitrobenzene crystals (Trotter, 1961*a*, *b*) has established the main features of the molecular structure: the carbon and nitrogen atoms all lie in one plane, but the nitro groups are twisted about 11° out of this plane. The bond distances and valency angles were, however, less precisely measured, and showed variations which were unlikely to be real. A full-matrix least-squares refinement (unpublished), in which a scale-factor parameter for each layer was refined, suggested that much of the trouble in obtaining satisfactory results might be associated with inaccuracies in the scale factors relating the various hkL layers ($L=0\rightarrow 3$), rather than in the refinement methods, and to overcome possible errors a new set of intensity data has now been measured by counter methods, and more accurate values of the bond distances and angles and of the thermal parameters have been obtained.

The cell parameters, remeasured on the General Electric Goniostat, are: $a=13{\cdot}257$, $b=14{\cdot}048$, $c=3{\cdot}806$ Å. The intensities of all 823 reflexions with $2\theta(\text{Cu } K\alpha)\leq 146°$ (minimum $d=0{\cdot}81$ Å) were measured with a scintillation counter, using the θ–2θ scan; 783 reflexions had intensities above background. The structure was refined by block-diagonal least-squares, minimizing $\Sigma w(|F_o|-|F_c|)^2$, with $\sqrt{w}=|F_o|/3$ when $|F_o|<3$ and $\sqrt{w}=1$ when $|F_o|\geq 3$. Hydrogen atoms were refined with isotropic, and the heavier atoms with anisotropic thermal parameters; the final R was 0·097 for the observed reflexions (structure factors are listed in Table 1, and comparison with the previous F_o values (Trotter, 1961*a*) indicates that the inter-layer scaling in the previous data contained inaccuracies). The final positional and thermal

* Alfred P. Sloan Foundation Fellow.